Journal of
Materials Chemistry B

Accepted Manuscript

This article can be cited before page numbers have been issued, to do this please use: W. Li, J. Wang, J. Zhu and Y. Zheng, *J. Mater. Chem. B*, 2018, DOI: 10.1039/C8TB01948G.

ROYAL SOCIETY OF CHEMISTRY

rsc.li/materials-b

View Article Online
DOI: 10.1039/C8TB01948G

Journal Name

ARTICLE

Co_3O_4 nanocrystals as an efficient catalase mimic for colorimetric detection of glutathione

Received 00th January 20xx,
Accepted 00th January 20xx

DOI: 10.1039/x0xx00000x

www.rsc.org/

Wenying Li,[a] Jiayan Wang,[b] Jiacheng Zhu,[b] Yue-Qing Zheng[a]*

Nanomaterial-based artificial enzymes (nanozymes), as an emerging generation of artificial enzymes, has received extensive attention in recent years owing to its striking merits. In this study, the obtained Co_3O_4 nanocrystals exhibited catalase-like activity, which could catalyze the oxidation of 3,3',5,5'-tetramethylbenzidine (TMB) in the presence of H_2O_2 and a clear absorption peak at 652 nm can be observed. It was verified that the catalytic activity for the oxidation of TMB originated from the oxygen, which is generated by Co_3O_4 catalyzed H_2O_2 decomposition. With the addition of glutathione (GSH), the catalytic ability of Co_3O_4 nanocrystals was inhibited. And the changes of absorbance at 652 nm could be utilized to quantify the concentration of GSH. Under the optimized conditions, the proposed assay showed good linear relationships and low detection limit towards GSH. Moreover, the Co_3O_4 nanocrystals had excellent stability and can keep the catalytic activity for a long time. Thus, a simple, sensitive and selective nanozyme-based biosensor was developed for colorimetric detection of GSH.

1. Introduction

Colorimetric assays have gained increasing research attention due to its simplicity, low cost and signal visibility.[1] An enzyme catalytic chromogenic reaction is frequently used to construct a colormetric assay since the enzyme possesses high catalytic efficiency and good specificity. However, natural enzymes are proteins or protein/RNA complexes, and the activities of them are easily affected by environmental conditions.[2] Therefore, significant interest has been devoted to constructing artificial enzymes in recent years. Of all the artificial enzymes, nanomaterial-based artificial enzymes (nanozymes) gained rapid development owing to their easy preparation, low cost, controllable structure and excellent catalytic activity. Inspired by these advantages, plenty of nanomaterials have been designed and synthesized to mimic the natural oxidase, peroxidase, catalase, and superoxide dismutase. [3-6]

Since the intrinsic peroxidase-like activity of magnetic Fe_3O_4 nanoparticles was discovered,[7] more and more efforts have been devoted on the development of nanozymes with enzyme-like activities for colorimetric detection of various targets.[3-5] It was found that many nanomaterials such as noble metal nanoparticles,[8, 9] metal oxide nanoparticles,[7,10-15] carbon nanomaterials[16], metal sulfide nanoparticles[17], metal phosphide nanoparticles[18], metal nitride nanoparticles[19], polymer nanoparticles[20], and hybrid nanoparticles[21-26] possess enzyme-like activities. Among these nanozymes, Co_3O_4 is believed to be a promising candidate for develop colorimetric assays since it possess several advantages such as excellent catalytic activity, good biological compatibility, wide band gap, high stability and low cost. Co_3O_4 nanoparticles is a kind of p-type semiconductor material with a band gap of about 2.1 eV, and has attracted considerable attentions in many fields. In 2012, Mu et al. reported that Co_3O_4 nanoparticles exhibited peroxidase-like activity and catalase-like activity.[10] After that, much research interest has been focused on the synthesis of cobalt-based nanomaterials with different morphology such as nanocubes, nanoplates, nanorods and nanowires. Also, the enzyme-liked activities of these nanomaterials with different morphology were studied. [12, 13, 18, 19]

Considering the practical applications of the nanozymes, researchers are always trying to obtain nanomaterials with excellent stability and catalytic activity. As for catalytic activity, construction of hybrid nanomaterials is an effective way to improve the catalytic performance.[21-26] In addition, it is known that size also has great effect on the catalytic performance of nanomaterials.[27] In general, the smaller the nanoparticle size is, the higher the catalytic activity is when the shape of the nanoparticle is the same. Therefore, another approach to obtain nanomaterials with excellent catalytic activity was to synthesize ultrasmall nanomaterials. However, the smaller metal oxides-based nanoparticles are very easy to aggregate for they have high surface area and surface energy,[28] which

[a] Research Center of Applied Solid State Chemistry, Chemistry Institute for Synhesis and Green Application, Ningbo University, Ningbo 315211, Zhejiang, PR China.
*Email: zhengyueqing@nbu.edu.cn.
[b] Medical School of Ningbo University, Ningbo 315211, Zhejiang, PR China.
†Electronic Supplementary Information (ESI) available: [details of any supplementary information available should be included here]. See DOI: 10.1039/x0xx00000x

View Article Online
DOI: 10.1039/C8TB01948G

have negative effects on the catalytic activities. In order to avoid the agglomeration, stabilizers such as surfactant can be added to disperse the nanoparticles. Though the introduction of surfactant is able to improve the stability of the nanomaterials, the presence of a surfactant is unfavorable for catalytic applications because the catalytic process takes place on the surfaces.[29] Therefore, much of our research interest has been directed to explore ultrasmall and surfactant-free nanostructures with good catalytic activities as enzyme mimic.

Notably, it was reported that Co_3O_4 quantum dots with ultrasmall size presented better visible light-driven oxygen evolution activities compared to the commercial Co_3O_4.[30] In addition, the Co_3O_4 quantum dots can be homogeneously dispersed in H_2O. However, to the best of our knowledge, no investigations have been performed on the enzyme-like catalysis activities of this ultrasmall Co_3O_4 nanocrystals. In this work, Co_3O_4 nanocrystals were prepared according to a reported method with little modification. The obtained Co_3O_4 nanocrystals can catalyze TMB to generate a typical blue color solution in the presence of H_2O_2, which seems like peroxidase-like properties. The mechanism of its catalytic activity was then investigated in detail. The results showed that the Co_3O_4 nanocrystals could accelerate H_2O_2 decomposition into oxygen, causing the oxidation of TMB, which demonstrated that the Co_3O_4 nanocrystals can be used as a catalase mimic. With the addition of GSH, concentration-dependent decrease in absorbance at 652 nm was observed. Based on these findings, a fast and facile colorimetric method was developed for the determination of GSH, and satisfactory results are obtained. It must be mentioned that the Co_3O_4 nanocrystals was extremely stable. In two months, no aggregation was observed and it was able to keep its catalytic activity.

2. Experimental

2.1 Materials and instrumentation

Cobalt(II) acetate tetrahydrate (99.5%) and benzyl alcohol were purchased from Aladdin Reagent Co., Ltd. (Shanghai, China). 30 nm Co_3O_4 nanopowder was purchased from Macklin Biochemical Co., Ltd. (Shanghai, China). 3,3',5,5'-tetramethylbenzidine (TMB), glutathione (GSH), cysteine (Cys), homocysteine (Hcy), glucose (Glu), uric acid (UA), xanthine (X) and Cytochrome *c* (Cyt *c*) were purchased from Sangon Biotechnology Co., Ltd. (Shanghai, China). Glycine (gly), serine (Ser), threonine (Thr), valine (Val), diethylenetriaminepentaacetic acid (DTPA) and terephthalic acid (TA) were purchased from Aladdin chemistry Co., Ltd. (Shanghai, China). Dihydroethidium (HE) was supplied by Sigma-Aldrich. Xanthine oxidase (XO) was purchased from Shanghai yuanye Bio-Technology Co., Ltd. Formaldehyde solution (37%~40%) was obtained from Sinopharm Chemical Reagent Co.,Ltd. All the chemicals were used as received.

Powder X-ray diffraction (XRD) patterns of the Co_3O_4 nanocrystals was obtained using D8 DISCOVER Plus diffractometer (Bruker, Germany). Transmission electron microscopy (TEM) high-resolution transmission electron microscopy (HRTEM) observations were performed on a JEM-2100 transmission electron microscope (JEOL, Japan). The X-ray photoelectron spectroscopy (XPS) was measured using an X-ray photoelectron spectrometer (ESCALAB 250Xi, Thermo Fisher) with a monochromatic Al Kα radiation source. The spectra were recorded for C1s, O1s, and Co2p levels with pass energy 20 eV and step 0.1 eV. The binding energies have been calibrated relative to C1s peak at 285.0 eV. The infrared spectra were recordedn a Shimadzu FTIR-8900 spectrometer in the range 4000 cm^{-1}–400 cm^{-1}.The dissolved oxygen was measured by using the NEOFOX-KIT-PROBE of Ocean Optics, an in-situ oxygen monitoring system.

UV–vis absorption spectrum were measured by using a 2501 UV–vis spectrophotometer (Shimadzu, Japan). Fluorescent measurements were recorded on a Shimadzu RF-5301 spectrophotometer with an excitation wavelength of 315 nm. Quartz cuvettes with 1-cm path length and 3 mL volume were used for the UV–vis and emission measurements. All the samples were prepared and measured at room temperature in a 10 mM acetate buffer (pH 5.0).

2.2 Synthesis of Co_3O_4 nanocrystals

Co_3O_4 nanocrystals were prepared by a published method with little modification. In a typical procedure, 160 mg Co(II) acetate and 7 ml benzyl alcohol were added to a round bottom flask. The mixture was stirred at room temperature until the solution become transparent. After that, 7 mL ammonium hydroxide (25%) solution was added dropwise into the flask under vigorous stirring. Then the flask was put into an oil bath adjusted at constant temperature of 165 °C. The solution was boiled immediately and after about 5 minutes the water condenser was installed. The reaction system was kept at 165 °C for 2 hours with stirring. Afterwards, the mixture was cooled to room temperature. Further, methyl tert-butyl ether was added to the reaction solution, affording a black precipitate. Finally, the black precipitate was collected by centrifugation and washed with ethanol. The Co_3O_4 nanocrystals (4 mg) was dispersed into distilled water (20 mL) to obtain a suspension of Co_3O_4 nanocrystals (200 μg mL^{-1})

2.3 Study of the catalytic activity of the Co_3O_4 nanocrystals

The effects that can affect the catalytic activities and the steady-state kinetics of the Co_3O_4 nanocrystals for the oxidation of TMB were studied by using the commonly used TMB/H_2O_2 system. A typical experiment was carried out by using 20 μg/mL Co_3O_4 nanocrystals with a total volume of 4 mL unless otherwise stated.

To examine the effects of Co_3O_4 nanocrystals on hydroxyl radical ($^{\bullet}OH$), 5 mM H_2O_2, 5 μM TA and different concentrations of the Co_3O_4 nanocrystals were first exposed to UV light 5 min. Then the a fluorescence spectrophotometer was used to record fluorescent spectra. To examine the effects of Co_3O_4 nanocrystals on superoxide radical ($^{\bullet}O_2^-$), 50 μM HE, 1 mM X, 0.1 mM DTPA, XO and Co_3O_4 nanocrystals was reacted for 30 minutes. Then the fluorescent spectra of the mixture was measured.

View Article Online
DOI: 10.1039/C8TB01948G

2.4 Assay procedures

The colorimetric assay system was prepared as follows: 200 μL of 10 mM acetate buffer (pH 5.0), 200 μL of TMB solution (5 mM, ethanol solution), 100 μL of 100 mM H_2O_2, 200 μL of 200 μg mL^{-1} Co_3O_4 nanocrystals, GSH and deionized water were added into cuvette, with the total volume of 2 mL. In this assay system, the final concentrations of GSH were 0, 5, 10, 20, 30, 40, 50 and 60 μM, respectively. The resultant mixture was incubated at room temperature for 5 min and then the absorbance spectroscopy was measured. For the interference experiments, 200 μL of the interfering analytes were added to the sample solution, and the final concentrations of the interfering analyte are all 40 μM.

3. Results and discussion

3.1 Characterization of the Co_3O_4 nanocrystals

The benzyl alcohol has already been shown to be suitable for the preparation of monodisperse metal-oxides nanoparticles, such as Fe_3O_4, Co_3O_4, Mn_3O_4, SnO_2 and In_2O_3.[31] And ultrasmall Co_3O_4 nanoparticles called Co_3O_4 nanocrystals was also reported by using benzyl alcohol as the solvent. We first prepared Co_3O_4 nanocrystals according this report. The XRD pattern of the obtained nanocrystals was shown in Fig. S1, and the XRD peaks can be well indexed to cubic phase Co_3O_4 (JCPDS No. 42-1467). The morphology of obtained Co_3O_4 nanocrystals was studied by using a transmission electron microscope (TEM), which is displayed in Fig. 1. As shown in Fig. 1a, the as-prepared Co_3O_4 nanocrystals shows a cube-like shape and is well-dispersed, which is in agreement with previous report. And the average size determined by TEM is 5 nm. Diffraction rings of selected-area electron diffraction could be indexed to theory values of the typical lattice planes, such as (220), (311) and (400) from cubicphase Co_3O_4. The HRTEM image (Fig. 1b) display a lattice spacing of 0.204 nm, which match well with the (440) lattice planes of Co_3O_4.[20] The elemental compositions and the oxidation states of the Co_3O_4 nanocrystals were further confirmed by XPS. The survey spectra of XPS (Fig. S2a) shows that the as-prepared Co_3O_4 nanocrystals only contains Co, O and C elements. The high-resolution Co 2p spectrum is shown in Fig. S2b, in which binding energies located at ~779.8 eV should be attributed to Co $2p_{3/2}$ and the small peak at~795.5 eV should be assign the ed to Co $2p_{1/2}$. The Co $2p_{3/2}$ and $2p_{1/2}$ peaks clearly shows that cobalt exist in a mixed-valence state of +2 and +3 in the obtained nanocrystals, which further confirms the existence of Co_3O_4.[32] Fourier transform infrared spectroscopy (FI-IR) test was carried out to verify the groups on the surface of the nanocrystals. As shown in Fig. S3, the strong band at 578 cm^{-1} and 666 cm^{-1} originated from Co – O stretching vibration of Co_3O_4. The broad band at 3385 cm^{-1} and the peak at 1650 cm^{-1} were ascribed to the O – H stretching vibration of the adsorbed H_2O molecules. The weak peak at 2920 cm^{-1} was assigned to the C – H of acetate ions, and the peaks at 1421 cm^{-1} and 1557 cm^{-1} could be attributed to C – O of acetate ions. The acetate ions are presumably conducive to the dispersion of Co_3O_4 nanocrystals in water according to previous report.[30]

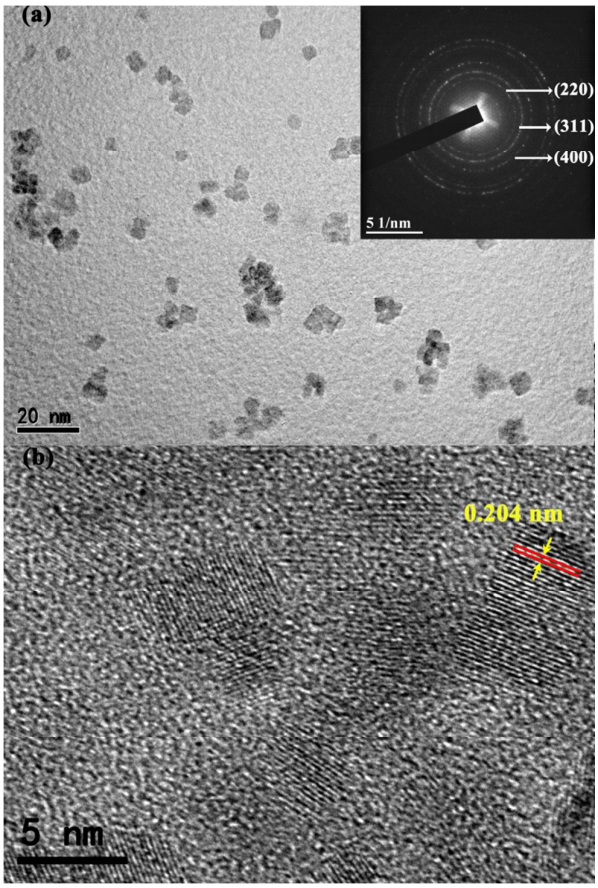

Fig. 1 (a) TEM image. Inset: SAED pattern. (b) HRTEM images of Co_3O_4 nanocrystals.

3.2 Investigation of catalytic activity of Co_3O_4 nanocrystals

Colorimetric systems were employed to further study on the catalytic activity of Co_3O_4 nanocrystals. TMB was chosen as the chromogenic substrate to investigate the enzyme-like activity of the Co_3O_4 nanocrystals. It is clearly from Fig. S4 that Co_3O_4 nanocrystals can catalyze the oxidation of TMB to generate a blue color solution and induce a significant absorbance change in the presence of H_2O_2. And it also can be seen from Fig. S4 that the Co_3O_4 nanocrystals could catalyze the the oxidation of TMB without H_2O_2, which means that the Co_3O_4 nanocrystals also possesses oxidase-like catalytic activity. And as is known, enzyme mimics like metal oxide are usually relative to pH and temperature. Firstly, the effects of pH on the catalytic ability of Co_3O_4 nanocrystals. Fig. S5 clearly shows that good catalytic activity could be obtained at the pH range form 4 to 6, and the highest absorbance was obtained at pH 5 for Co_3O_4 nanocrystals. Therefore, buffer with pH of 5.0 is used in the following experiments. Then the effects of temperature on the catalytic ability of Co_3O_4 nanocrystals was investigated. As shown in Fig. S6, the Co_3O_4 nanocrystals all possess catalytic ability over a wide range from 0 °C to 50 °C, and the optimal temperature is 40 °C. Nevertheless, we used room temperature (25 °C) in the following studies of this work for convenience. Besides, the stability of the Co_3O_4 nanocrystals was also studied. It can be seen form Fig. S7 that no aggregation was observed after 2 months and and the catalytic activity of Co_3O_4 nanocrystals after 2 months is almost the same with freshly prepared. It was shown in Fig. S3 that

View Article Online
DOI: 10.1039/C8TB01948G

acetate ions existed in the infrared spectroscopy of Co_3O_4 nanocrystals, and we infer that the excellent stability can be can be attribute to the acetate ions that are helpful to the dispersion of Co_3O_4 nanocrystals in water. Unfortunately, there are still no clear answers to the reaction mechanism. When placed into a solution with the TMB and H_2O_2 added, Co_3O_4 nanocrystals can induce a continued increase in absorbance change at 652 nm. Since the absorbance increases with time linearly in 5 minutes (Fig. S8, line 1), we chose reaction time of 5 minutes to do the following studies. And it also can be seen from from Fig. S8 that the Co_3O_4 nanocrystals exhibited superior catalytic acitivity compared with the commerical 30 nm Co_3O_4 (Fig. S8, line 1 and line 2). It is proposed that the improved activity of the Co_3O_4 nanocrystals can be attributed to the excellent dispersibility and small size, which inevitably resulted in significant increases in specific surface area as well as reactive sites. In addition, the enzyme-like activity of Co_3O_4 nanocrystals was also dependent on the amount of Co_3O_4 (Fig. S9).

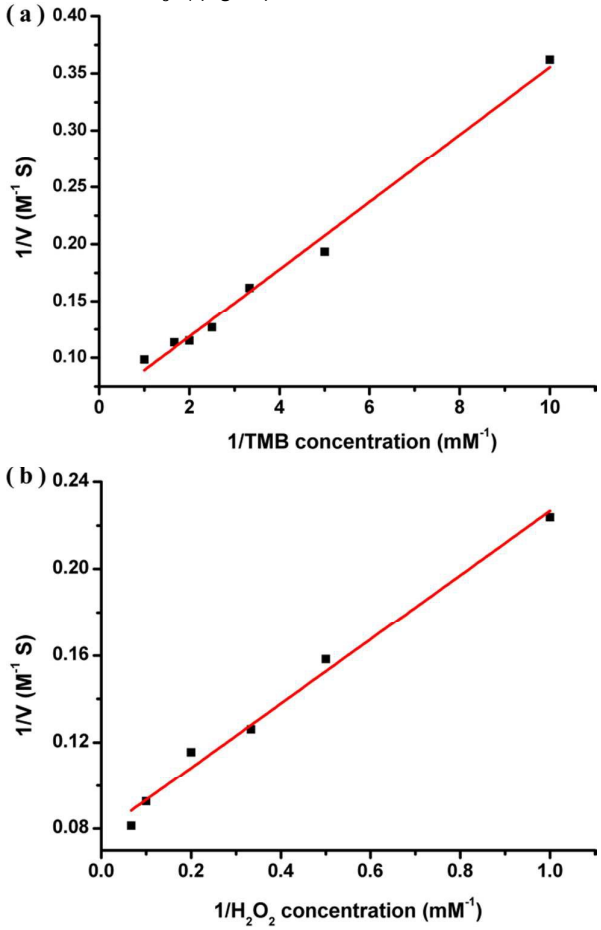

Fig. 2. Steady-state kinetic assay. (a) Double reciprocal plots of activity of Co_3O_4 nanocrystals with the concentration of TMB varied. The TMB concentration was 0.1, 0.2, ,0.3, 0.4, 0.5, 0.6, 1.0 mM, respectively. (b) Double reciprocal plots of activity of Co_3O_4 nanocrystals with the concentration of H_2O_2 varied. The H_2O_2 concentration1, 2, 3, 5, 10, 15 mM, repectively.

Morever, to better understand the enzyme-like activity of Co_3O_4 nanocrystals, the steady-state kinetics was studied by varying the concentration of TMB or H_2O_2 and fixing the other (Fig. S10). The kinetic parameters of the catalytic oxidation reaction are determined by fitting the data of Fig. S10 into Michaelis-Menten equation. A molar absorption coefficient of 39 000 M^{-1} cm^{-1} for TMB was used to calculate the initial velocity. Michaelis constant (Km) is usually used as an indicator of enzyme affinity to substrates, which can be obtained from the Lineweaver-Burk plots. Table S1 showed that the Km values obtained with TMB as substrate from Fig. 2a was 0.49 mM, comparable with that of horseradish peroxidase. And the Km value of Co_3O_4 nanocrystals with H_2O_2 as substrate was 1.9 mM (Fig. 2b), suggesting that Co_3O_4 nanocrystals has higher affinity for H_2O_2 than HRP.[7,17]

In addition, to confirm the catalytic mechanism of Co_3O_4 nanocrystals, two different fluorescent probes terephthalic acid (TA) and dihydroethidium (HE) were applied to the detection of hydroxyl radical ($^{\bullet}OH$) and superoxide radical ($^{\bullet}O_2^-$), respectively. TA could easily react with $^{\bullet}OH$ to generate highly fluorescent compound.[33] A decrease of the fluorescence intensity was observed as the concentration of Co_3O_4 nanocrystals continue to increase (Fig. S11), which indicated that Co_3O_4 had $^{\bullet}OH$ scavenging activity rather than contributed to formation of $^{\bullet}OH$. The emission intensity of HE, which could react with $^{\bullet}O_2^-$ to produce fluorescent ethidium[34], decreased in the presence of Co_3O_4 nanocrystals (Fig. S12), suggesting that the Co_3O_4 nanocrystals reduced the formation of $^{\bullet}O_2^-$. Together, these results revealed that the nature of the catalytic activity of Co_3O_4 nanocrystals was not originate from $^{\bullet}OH$ generation nor $^{\bullet}O_2^-$ generation. Furthermore, dissolved oxygen concentrations in H_2O_2 decomposition with the addition of Co_3O_4 nanocrystals was recorded by using an in-situ oxygen monitoring system (Fig. 3). The results strongly suggested that the Co_3O_4 nanocrystals showed catalase-like catalytic activity that could accelerate H_2O_2 decomposition into oxygen, and the activity of Co_3O_4 nanocrystals for the oxidation of TMB originated from the production of oxygen.

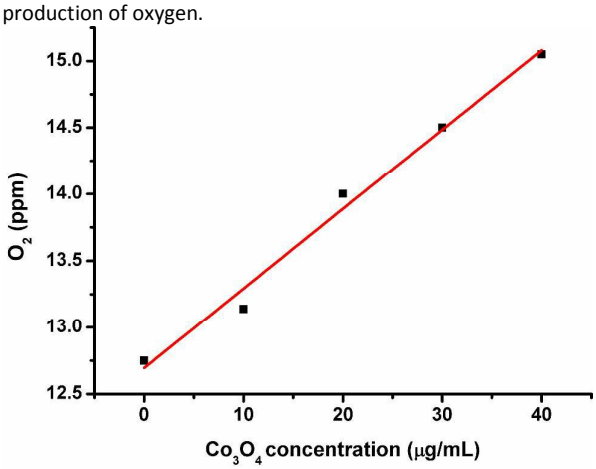

Fig. 3. Effect of the Co_3O_4 nanocrystals concentration on the generation of O2 by decomposition of H_2O_2. Reaction conditions: 5 mM H_2O_2 and different concentrations of nanocrystals (pH 5.0).

Besides, to rule out the possibility that the Co_3O_4 nanocrystals directly worked as electron transfer mediators, the oxidation of Cyt *c* was tested. The two peaks of the α band of Cyt *c* in a reduced state disappeared in the presence of Co_3O_4 nanocrystals, and a new peak at 530 nm appeared, which indicating Cyt *c* was oxidized (Fig. S13)[12]. To examine the effect of O_2 in the Cyt *c* oxidation reaction, all the solutions were purged with high purity N_2 for 0.5 h and then

View Article Online
DOI: 10.1039/C8TB01948G

mixed together. nitrogen for 0.5 h and then repeated the same process. The results showed that spectral changes were very little, confirming that the oxidation of Cyt *c* by Co_3O_4 rely on the dissolved oxygen.

3.3 GSH detection using Co_3O_4 nanocrystals

GSH is a thiolated tripeptide and involved in many processes in the body. It is produced naturally by the liver and its level is closely related to a number of diseases, such as liver damage, cancer and senile dementia.[21, 24, 25, 35] In this work, a simple, rapid and sensitive colorimetric sensing assay was developed for GSH detection based on the catalase-like catalytic activity of the Co_3O_4 nanocrystals.

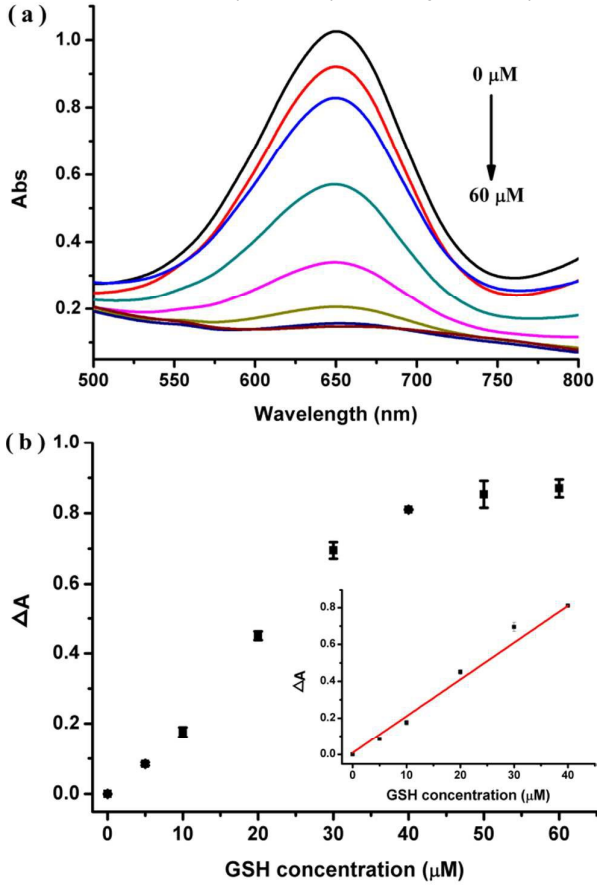

Fig. 4 (a) Changes in the absorbance of Co_3O_4-H_2O_2-TMB system upon the addition of GSH with different concentrations. (b) The decrease of the absorbance (ΔA) at 652 nm versus concentrations of GSH. Inset: expanded linear region of the calibration curve. Assay conditions: 0.5 mM TMB, 5 mM H_2O_2, pH 5.0, 20 μg/mL Co_3O_4 nanocrystals.

As presented in Fig. 4, the absorption spectra of TMB decreased significantly as the concentration of GSH increased from 0 – 40 μM. With more GSH added, only little change in the absorbance could be observed. The results indicated that up to 40 μM GSH can be detected with 20 μg/mL of Co_3O_4 nanocrystals. The absorbance at 652 nm is proportional to the GSH concentration in the range 0 – 40 μM. The linear regression equation is: $\Delta A = 0.02c + 0.01$ (R^2=0.99), in which ΔA represent the change of absorbance at 652 nm and c is the concentration of GSH. The detection limit of the assay was calculated according to the standard deviation of six blank (σ) sample and the slope of the calibration curve (K), was found to be 500 nM (3σ/K). Trough the comparison of analytical performances between our proposed assay and other GSH detection method in recent years, it was found that our method has an acceptable sensitivity.[21, 24, 25, 35]

In order to clarify the reason why GSH can inhibit the TMB color reaction, a series of experiments was performed. Firstly, 40 μM GSH was added to an oxidized TMB solution which was obtained by UV irradiation of a mixed solution of TMB and H_2O_2. As shown in Fig. S14, dramatic decrease in the absorbance was observed. With the addition of 40 μM GSH, the absorbance at 652 nm here dropped 75% while 79% in Fig. 4, which demonstrated that the redox reaction between GSH and oxTMB should be a main reason of the inhibition of color reaction. Secondly, to assesses the possibility that the Co_3O_4 was directly reacted with GSH, Co_3O_4 was mixed with GSH for 30 minutes and then the Co_3O_4 was recollected after centrifugation, washing and drying. Then a comparison of the catalytic activity was made between Co_3O_4 nanocrystals pretreated by GSH and Co_3O_4 without pretreatment. As shown in Fig. S15, pretreatment with GSH only has little influence on the catalytic activity of Co_3O_4. We further performed XPS measurements, and no obvious valence changes of the nanocrystal after GSH treatment can be observed Fig. S16. The above results indicated that the inhibition of TMB color reaction was mainly resulted from the redox reaction that take place between GSH and the direct interaction between GSH and Co_3O_4 nanocrystals accounted for only a small part of the inhibition.

3.4 Selectivity of the assay

Excellent selectivity is also a significant requirement for a good assay. To investigate the selectivity of this Co_3O_4 nanocrystals based assay, various potential components were studied, including metal ions (K^+, Na^+, Mg^{2+}, Mn^{2+}, Zn^{2+}) and amino acids (Cys, Hcy, Gly, Ser, Thr, Val), glucose (Glu) and uric acid (UA). As illustrated in Fig. 5a, it was obvious that GSH could significantly inhibited the catalytic activity of the Co_3O_4 nanocrystals while very little interference could be observed with the addition of some metal ions (K^+, Na^+, Mg^{2+}, Mn^{2+}, Zn^{2+}), some amine acids (Gly, Ser, Thr, Val), glucose or uric acid. Photograph of the selectivity was presented in Fig. 5b, and it can be seen that the sample with GSH added was colorless while other samples blue. In addition, it should point out that Cys and Hcy exhibit considerable inhibition of catalytic activity. On account of that the amino acids with thiol-group can cause some interference, 1 μL commercial formaldehyde solution (37%~40%) was added to the interfering substances (Cys, Hcy and a mixture of above mentioned interferents). And after two minutes, the reaction solution was added to our colorimetric assay system and reacted for another 5 minutes before its absorbance was measured. As shown in Fig. 5c, it was found that the effect of Cys, Hcy and the mixture of above mentioned interferents is almost negligible by the pretreatment with formaldehyde solution. These results indicated that the method was selective for GSH detection.

View Article Online
DOI: 10.1039/C8TB01948G

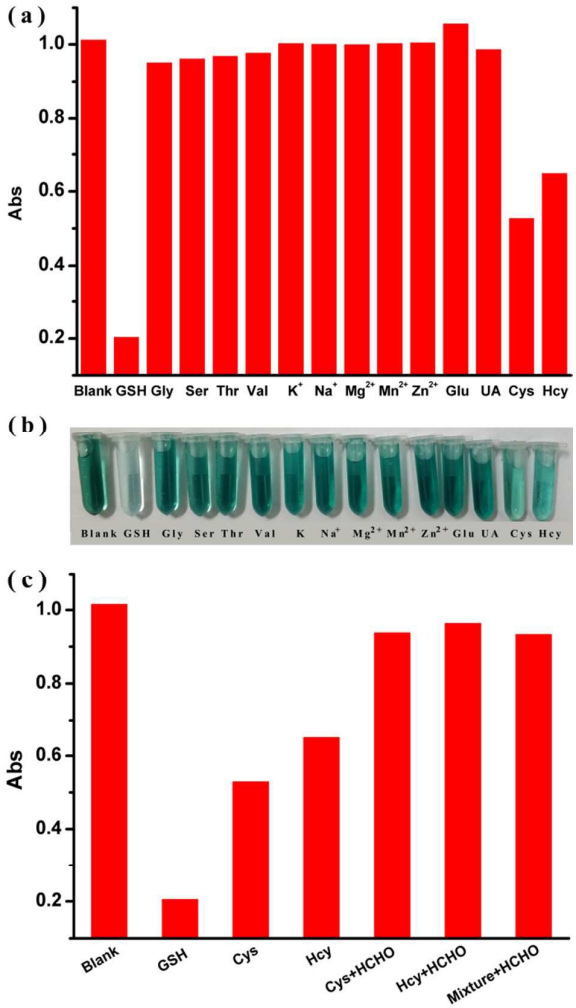

Fig. 5 Selectivity of the colorimetric methods for GSH detection. Assay conditions: 0.5 mM TMB, 5 mM H_2O_2, pH 5.0, 20 μg/mL Co_3O_4 nanocrystals, 40 μM GSH or other interferences.

3.5 Analysis of real samples

The feasibility of the assay in real samples was evaluted by analyzing GSH in diluted serum examples. For more validation, known volumes of GSH standard solution was added into the diluted serum examples, and the recovery values and RSD values were calculated. Herein, the serum examples was diluted to make sure that the GSH concentration are in the linenar range, and incubated with formaldehyde solution for two minutes. The obtained results are shown in Fig. S17 and summarized in Table 1. As shown in Table 1, the GSH in the diluted serum was determined to be 1.020 μM, which was in the same level compared to previous report. This can be explained by the fact that cysteine also existed in serum and it had larger effect on GSH detection compared with other interference. Moreover, 96.00% to 109.7% recoveries with a RSD ranging from 3.5% to 4.9% are observed in the spiked serum samples with three different concentrations of GSH, which indicated that our assay can be successfully used for GSH detection in real examples.

Table 1 Results of GSH detection in serum sample.

Added(μM)	Founded(μM)	Recovery(%)	RSD(N=3,%)
0	1.020		3.5
2	2.940	96.00	4.2
10	11.99	109.7	4.9
20	22.37	106.8	3.8

Throughout this work, we can see that our study has several distinct features: First, the catalytic acitivity of the ultrasmall and surfactant-free Co_3O_4 nanocrystals was studied for the first time. Second, the Co_3O_4 nanocrystals was found to be ultrastable and its catalytic activity remained essentially unchanged in two months. Third, the interference of Cys and Hcy which often existed in GSH sensing was eliminated here. Forth, our method is easy to operate and time-saving, and it can be said that it is a 'mix-and-detect' approach for GSH detection.

4. Conclusions

In the present work, a simple and selective assay was constructed for determination of GSH based on catalase-like catalytic activity of ultrasmall Co_3O_4 nanocrystals. The enzyme-like catalytic activity and the catalytic mechanism were studied in detail. GSH could inhibit the oxidation of TMB and caused a decrease in the absorbance. The decrease of the absorbance at 652 nm was directed related to the amount of GSH added. And a limit of detection of 500 nM was achieved. We envision that that this kind of metal oxide nanocrystals could be utilized as an efficient catalase mimic for biological detection.

Conflicts of interest

There are no conflicts to declare.

Acknowledgements

This work was financially supported by the Natural Science Foundation of Zhejiang Province (LQ17B040001), Natural Science Foundation of Ningbo (2017A610235), Open Research Fund of State Key Laboratory of Electroanalytical Chemistry (SKLEAC201804), Ningbo University Research Programs (421608940, 421703840, XYL17018, 421707650) and the K. C. Wong Magna Fund in Ningbo University.

Notes and references

1 S. Cai, C. Qi, Y. Li, Q. Han, R. Yang and C. Wang, *J. Mater. Chem. B*, 2016, **4**, 1869.
2 Y. Lin, J Ren, X. Qu, *Acc. Chem. Res.*, 2014, **47,** 1097.
3 H. Wei and E. K. Wang, *Chem. Soc. Rev.*, 2013, **42**, 6060.
4 X. Wang, Y. and H. Wei, *Inorg. Chem. Front.*, 2016, **3**, 41.
5 Shi. Liu, L. Han, N. Li, N. Xiao, Y. Ju, N. Li and H. Luo, *J. Mater. Chem. B*, 2018, **6**, 2843.
6 N. Singh, M. A. Savanur, S. Srivastava, P. D'Silva and G. Mugesh, *Angew. Chem. Int. Ed.*, 2017, **56**, 1427.
7 L. Gao, J. Zhuang, L. Nie, J. Zhang, Y. Zhang, N. Gu, T. Wang, J. Feng, D. Yang, S. Perrett and X. Yan, *Nat. Nanotech.*, 2007, **2**, 577.

View Article Online
DOI: 10.1039/C8TB01948G

8 Y. Hu, H. Cheng, X. Zhao, J. Wu, F. Muhammad, S. Lin, J. He, L. Zhou, C. Zhang, Y. Deng, P. Wang, Z. Zhou, S. Nie and H. Wei, *ACS Nano*, 2017, **11**, 5558.
9 W. Zhang, X. Niu, X. Li, Y. He, H. Song, Y. Peng, J. Pan, F. Qiua,, H. Zhao and M. Lan, *Sens. Actuator B-Chem*, 2018, **265**, 412.
10 A. A. Vernekar, D. Sinha, S. Srivastava, P. U. Paramasivam, P. D,Silva and G. Mugesh, *Nat. Commun.*, 2014, **5**, 5301.
11 J. Mu, Y. Wang, M. Zhao and L. Zhang, *Chem. Commun.*, 2012, **48**, 2540.
12 J. Dong, L. Song, J.-J. Yin, W. He, Y. Wu, N. Gu and Y. Zhang, *ACS Appl. Mater. Interfaces*, 2014, **6**, 1959.
13 J. Mu, L. Zhang, M. Zhao and Y. Wang, *ACS Appl. Mater. Interfaces* 2014, **6**, 7090.
14 J. Liu, L. Meng, Z. Fei, P. J. Dyson, X. Jing, X. Liu, *Biosen. Bioelectron.*, 2017, **90**, 69.
15 X. Niu, Y. He, W. Zhang, X. Li, F. Qiu and J. Pan, *Sens. Actuator B-Chem*, 2018, **256**, 151.
16 Y. Song, X. Wang, C. Zhao, K. Qu, J. Ren and X. Qu, *Chem. Eur. J.,* 2010, **16**, 3617.
17 X. Niu, Y. He, J. Pan, , X. Li, F. Qiu, Y. Yan, L. Shi, H. Zhao and M. Lan, *Anal. Chim. Acta*, 2016, **947**, 42.
18 Y. He, F. Qi, X. Niu, W. Zhang, X. Zhang and J. Pan, *Anal. Chim. Acta*, 2018, **1021**, 113.
19 Y. Li, T. Li, W. Chen and Y. Song, *ACS Appl. Mater. Interfaces*, 2017, **9**, 35.
20 Z. Yang, C. Wang and X. Lu, *Sci. China Mater.*, 2018, **61**, 653.
21 M. Chi, S. Chen, M. Zhong, C. Wang and X. Lu, *Chem. Commun.*, 2018, **54**, 5827.
22 Y. Jiang, N. Song, C. Wang, N. Pinna and X. Lu, *J. Mater. Chem. B*, 2017, **5**, 5499.
23 W. Song, M. Chi, M. Gao, B. Zhao, C. Wang and X. Lu, *J. Mater. Chem. C*, 2017, **5**, 7465.
24 W. Zhu, M. Chi, M. Gao, C. Wang, X. Lu, *J. Colloid Interface Sci.*, 2018, **528**, 410.
25 Y. Yang, L. Shi, H. Zhao, M. Lan, W. Yang, J. Hao, Z. Zhang and B. Zhang, *New J. Chem.*, 2015 , **39**, 8802.
26 H. Zhao, Y. Dong, P. Jiang, G. Wang and J. Zhang, *ACS Appl. Mater. Interfaces* 2015, **7**, 6451.
27 Y. Peng, Z. Wang, W. Liu, H. Zhang, W. Zuo, H. Tang, F. Chen and B. Wang, *Dalton Trans.*, 2015, **44**, 12871.
28 X. Yu, S. Tong, M. Ge, J. Zuo, C. Cao and W. Song, *J. Mater. Chem. A*, 2013, **1**, 959.
29 A. A. Vernekar, T. Das, S. Ghosh and G. Mugesh, *Chem. Asian J.,* 2016, **11**, 72.
30 N. Shi, W. Cheng, H. Zhou, T. Fan and M. Niederberger, *Chem. Commun.*, 2015, **51**, 1338.
31 N. Pinna and M. Niederberger, *Angew. Chem. Int. Ed.*, 2008, **47**, 5292.
32 A. Indra, P. W. Menezes, C. Das, C. Göbel, M. Tallarida, D. Schmeiber and M. Driess, *J. Mater. Chem. A*, 2017, **5**, 5171.
33 A. Hua, H. Denga, X. Zheng, Y. Wu, X. Lin, A. Liu, X. Xia, H. Peng, W. Chen and G. Hong, *Biosen. Bioelectron.*, 2017, **97**, 21.
34 H. Zhao, S. Kalivendi, H. Zhang, J. Joseph,K. Nithipatikom, J. Vásquez-Vivar and B. Kalyanaraman, *Free Radic. Biol. Med.*, 2003, **34**, 1359.
35 Y. Zhang, W. Zhang, K. C., Q. Yang, N. Hu, Y. Suo and J. Wang, *Sens. Actuator B-Chem*, 2018, **262**, 95.

View Article Online
DOI: 10.1039/C8TB01948G

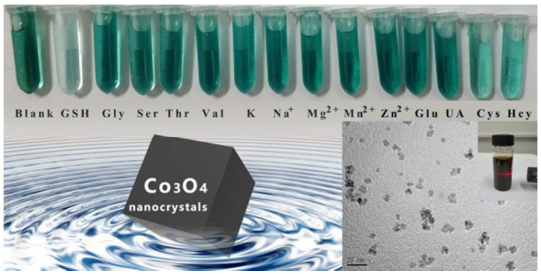

Co_3O_4 nanocrystals with ultrasmall size, excellent satability and catalytic activity was used as an efficient catalase mimic.